Design of a New Signal Structure for Active Sensing in Cognitive Radio Systems

Han-Wei Chen
Institute of Communications Engineering
National Tsing Hua University
Hsinchu, Taiwan 30013, R.O.C
d9564820@oz.nthu.edu.tw

Chin-Liang Wang
Department of Electrical Engineering and
Institute of Communications Engineering
National Tsing Hua University
Hsinchu, Taiwan 30013, R.O.C
clwang@ee.nthu.edu.tw

***Abstract*—Spectrum sensing is one of the major elements of cognitive radio (CR) systems. The periodic spectrum sensing frame structure can provide reliable sensing agility by introducing sensing quiet periods among signal frames to protect the primary users (PUs) from interference. However, arranging too many intra-frame sensing quiet periods on CR signaling may degrade the quality of service (QoS) of the CR network. To solve this problem, active sensing, performing spectrum sensing and transmitting data simultaneously, has been proposed to replace the intra-frame sensing. One drawback of active sensing is that the sensing performance becomes limited due to the interference from CR network transmissions. In this paper, a new CR signal structure for active sensing based on the cyclostationary properties is proposed, with which the active sensing performance can be further improved while maintaining the QoS of the CR system. Simulation results show that the proposed method significantly improves the detection performance of active sensing, especially when the signal strength from PUs is sufficiently low.**

I. Introduction

In recent years the wireless spectrum is in high demand due to the flourishing development of new wireless services. However, the wireless spectrum is a finite resource. Cognitive radio (CR) [1], a special type of software-defined radio, has been proposed to solve the spectrum scarcity. The CR system accesses the licensed spectrum for its transmission in an opportunistic way and causes no interference to primary users (PUs). In order to prevent PUs from interference, it is essential for the CR system to perform spectrum sensing periodically.

A proposal about periodic spectrum sensing frame structure has been accepted in IEEE 802.22 Working Group [2] and is illustrated in Fig. 1(a), where a superframe consists of 16 frames; each frame is divided into data transmission period and quiet sensing period. During the quiet periods, the transmissions of all CR users are suspended to ensure the accuracy of sensing results. The media access control (MAC) layer of the CR system dynamically and adaptively schedules the quiet periods to allow the system balance quality of service (QoS) requirements of users. Obviously, the sensing performance is improved by an increase in the number of quiet periods, but too many intra-frame sensing quiet periods on CR signaling may degrade the QoS of the CR network.

The characteristics and fundamental problems of the periodic sensing frame structure have been discussed in [3] and [4]. The authors of [5] and [6] proposed the idea of active sensing to replace intra-frame sensing quiet periods. The mechanism of active sensing is illustrated in Fig. 1(b) where the CR network performs spectrum sensing and data transmission simultaneously, so that quiet periods of intra-frame sensing can be saved. Although active sensing maintains the QoS of CR network, the mixed signal (PU and CR signals) worsens the conditions to detect the signals of PU. An ordinary detector (e.g., energy detector) is not robust to the noise and interferences; thus, the sensing performance was restricted by the interference from CR network transmissions.

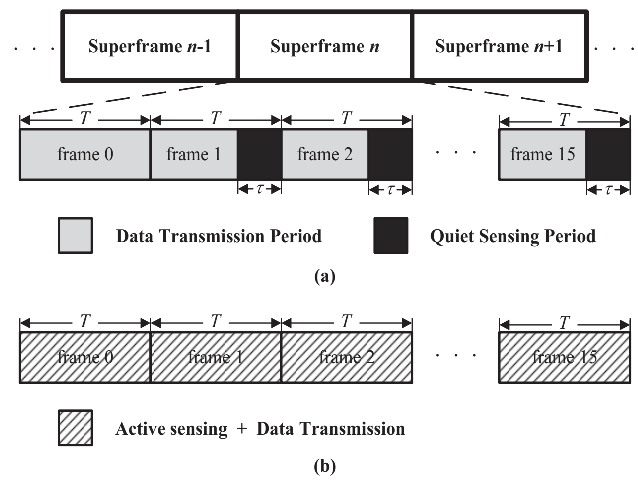

Fig. 1. The CR frame structures with spectrum sensing. (a) Periodic spectrum singing frame structure. (b) Active sensing frame structure.

Many communication signals in use today can be modeled as cyclostationary signals because of the presence of one or more underlying periodicities. Those signal periodicities can be detected through cyclostationary signal analysis [7]. In this paper a new signal structure for active sensing based on the cyclostationary properties is presented. We duplicate the PU's pilot signals and insert to the CR signals intentionally to generate similarity patterns between PU and CR signals. Therefore, when the CR network and PU network are both active, an intentional cyclostationary feature occurs and is noted by performing a cyclostationary signal analysis test.

978-1-4673-0990-5/12/$31.00 ©2012 IEEE

II. System Model

Consider a centralized CR network, as depicted in Fig.2, some of the CR users are actively transmitting data with the CR base station; others are inactive as spectrum sensing nodes, performing active sensing and monitoring the status of PU networks continuously. A binary hypothesis is defined where $\mathcal{H}_0$ and $\mathcal{H}_1$ represent the absence and presence of the primary signals, respectively. Assume the PU and CR are orthogonal frequency division multiplexing (OFDM) based systems; the signals of PU and CR systems in the time domain can be denoted by $s^p_{n,l}$ and $s^c_{n,l}$, where n is the sample index and l is the symbol index of the OFDM signal. As for the signal received by active-sensing nodes, $r_{n,l}$, the input-output relation is given as

$$\begin{cases} \mathcal{H}_1: & r_{n,l} = h^p_{n,l} \cdot s^p_{n,l} + h^c_{n,l} \cdot s^c_{n,l} + w_{n,l} \\ \mathcal{H}_0: & r_{n,l} = h^c_{n,l} \cdot s^c_{n,l} + w_{n,l} \end{cases} \tag{1}$$

where $w_{n,l}$ indicates an additive complex white Gaussian noise with zero mena and variance σ^2_w, i.e., $w[n] \sim \mathcal{CN}(0, \sigma^2_w)$; $h^p_{n,l}$ and $h^c_{n,l}$ are the temporary channel gains of the signal that the active-sensing nodes received from the CR network and from the PU network, respectively. In the frequency domain, the received signal at k_{th} subband of l_{th} OFDM symbol can be represented by its discrete-time Fourier transform (DFT) as

$$R_{k,l} = \frac{1}{\sqrt{N}} \sum_{n=0}^{N-1} r_{n,l} \cdot e^{-j2\pi nk/N}. \tag{2}$$

Thus, we have

$$\begin{cases} \mathcal{H}_1: & R_{k,l} = H^p_{k,l} \cdot S^p_{k,l} + H^c_{k,l} \cdot S^c_{k,l} + W_{k,l} \\ \mathcal{H}_0: & R_{k,l} = H^c_{k,l} \cdot S^c_{k,l} + W_{k,l} \end{cases} \tag{3}$$

where $H^p_{k,l}$ and $H^c_{k,l}$ are the equivalent baseband channel frequency responses of the signal from the PU and CR networks; $S^c_{k,l}$ and $S^c_{k,l}$ are the transmitted signals from PU and CR systems, while W_k is the received noise represented in the frequency domain. In equation (3), under the hypothesis $\mathcal{H}_1$, the PU and CR networks are both active, and the active-sensing nodes can also sense the signals transmitted by neighboring CR users, which caused severe conditions to sense the signals from the PU. A common detector (e.g., energy detector) cannot provide robust sensing under the condition [5].

A cyclostationary feature detector has the ability to extract the PU's features from mixed signals and, thus, is a suitable detector for active sensing. The cyclostationary signal analysis, using the spectral correlation function (SCF) proposed by [7], measures the similarity of a spectrum to a nearby spectrum. In an OFDM-based system, the time-smoothed spectrum similarity pattern $\bar{\Gamma}^{\alpha}_{x}[k]$ can be obtained through the spectral correlation function [8]

$$\bar{\Gamma}^{\alpha}_{x}[k] = \frac{1}{L} \sum_{l=0}^{L-1} X_{k,l} \cdot X^*_{(k-\alpha),l} \cdot H^{sm}_k \tag{4}$$

where $X_{k,l}$ is the discrete Fourier transform of the received signal $x_{n,l}$, and H^{sm}_k denotes a smoothing spectral window.

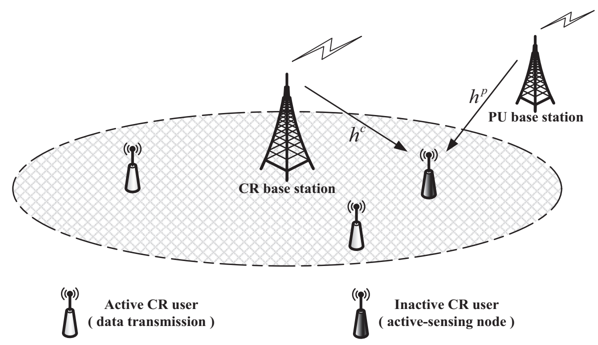

Fig. 2. The active sensing scenario of this paper.

Equation (4) specifies the similarity pattern that occurs when the signal spectrum in different frequencies are alike. The inherent three dimensions (frequency-frequency-intensity) of the SCF test would explore, identify and classify the blended signals in active sensing. Although the cyclostationary signal analysis provides high accuracy for spectrum sensing, the computational complexity is extremely high when evaluating $\bar{\Gamma}^{\alpha}_{x}[k]$ for each spectrum frequency k over all cyclic frequencies α.

III. The Proposed Active Sensing Method

A. A New Signal Structure

The objective to the design of CR's signal structure is embedding intentional cyclostationary features in the received signal $r_{n,l}$ through an exceptional data deployment of CR. The intentional features can be generated by deploying the same data on two or more subcarriers of the signal. The intentional cyclostationary features can be regarded as predictable features if the indices of subcarriers which carry the same data source are known by the receivers and, thus, the task left for the sensing nodes is detecting those spectrum similarity features. This method could significantly reduce the computational complexity of the SCF test if the subcarriers' frequencies carrying the same data are known at the sensing nodes.

Now we consider the active sensing case under $\mathcal{H}_1$, where PU and CR networks are both active within the same band; the blended signals, which are composed of CR signals and PU signals, are received by active-sensing nodes of the CR system. Assume that the PU is a pilot-embedded system (e.g., OFDM systems), and that the signal structure of the PU system is known by the active-sensing nodes; that is, the OFDM-based CR system knows the pilot information of the PU system. These assumptions are sensible because the PU system is a public digital television broadcasting system according to IEEE 802.22.

After the pilot information is known by the CR systems, the transmitters in the CR network can insert the same pilot value as the PU signals into some of the subcarriers of its signal. When the PU and CR networks are both active, the intentional features of the blended signals can be easily detected by the

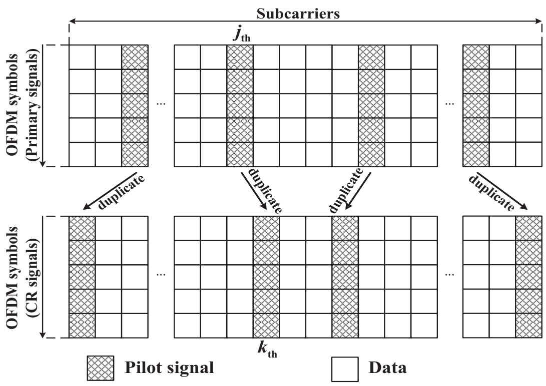

Fig. 3. Proposed signal structure for active sensing in cognitive radio.

active-sensing nodes by using the SCF test in equation (4). The data deployment procedure of the proposed method is duplicating the PU's pilot values and inserting the pilot values to one or more frequency subcarriers of the CR signals. The concept of the proposed method is shown in Fig. 3. The horizontal axis and the vertical axis represent, individually, the subcarriers and OFDM symbols of the PU and the CR signals in the frequency domain. In the PU's signal, the subcarriers with oblique lines are the pilot tones. Duplicating the pilot value of the j_{th} subcarrier of the PU's signal, the users of the CR system insert the pilot value into the k_{th} subcarrier of its own signals; that is

$$S^c_{k,l} = S^p_{j,l}, \text{ for all symbols, } l; \tag{5}$$

Under $\mathcal{H}_1$, the received signals are

$$R_{j,l} = H^p_{j,l} \cdot S^p_{j,l} + H^c_{j,l} \cdot S^c_{j,l} + W_{j,l}, \tag{6}$$

$$R_{k,l} = H^p_{k,l} \cdot S^p_{k,l} + H^c_{k,l} \cdot S^c_{k,l} + W_{k,l}. \tag{7}$$

We can find that $S^c_{j,l}$ and $S^p_{k,l}$ are the subcarriers carrying the data of PU and CR systems; they can be viewed as random sequences and are mutually independent. Therefore, an cyclostationary feature Γ_R^{k-j} occurs through $(R_{k,l} \cdot R^*_{j,l})$ due to the correlated $S^c_{k,l}$ and $S^p_{j,l}$. If the PU network and the CR network are active at the same time, the similarity features will surely appear in the blended signals. If the PU network is not active, the similarity features generated by our method will no longer exist because the portion in the j_{th} frequency from PU's pilot signals is not available.

B. A Signal Detection Algorithm

In this subsection, we provide an active sensing algorithm dedicated to the proposed signal structure. Segmenting the received baseband signal samples with a length of N_s, the active sensor averages every M segment in the time domain to eliminate the effect of noise,

$$\overline{r}_n = \frac{1}{M}\sum_{l=0}^{M-1} r_{n,l}, \ n = 0, 1, ..., N_s - 1, \tag{8}$$

where the overline refers to the averaged sequence. N_s is a complete OFDM symbol duration of the CR system, including the cyclic prefix. Then $\overline{R}_k$, the N_s-point discrete Fourier transform (N_s-DFT) of $\overline{r}_n$, will be

$$\overline{R}_k = \sum_{n=0}^{N_s-1} \overline{r}_n e^{-j2\pi kn/N_s} = \frac{1}{M}\sum_{l=0}^{M-1} R_{k,l} \tag{9}$$

Under H_1, $\overline{R}_k$ can be expressed as

$$\overline{R}_k = \frac{1}{M}\sum_{l=0}^{M-1}\{H^p_{k,l}S^p_{k,l}e^{j\phi^p_{k,l}} + H^c_{k,l}S^c_{k,l}e^{j\phi^c_{k,l}} + I_{k,l} + W_{k,l}\} \tag{10}$$

where $I_{k,l}$ represents the total of inter-symbol interference (ISI) and inter-carrier interference (ICI), $e^{j\phi_{k,l}}$ is the phase rotation resulting from timing synchronization error, and $W_{k,l}$ is the complex Gaussian noise. For convenience, let us rewrite equation (10) in a simpler form,

$$\overline{R}_k = \{\hat{S}^p_k + \hat{S}^c_k + \hat{I}_k + \hat{W}_k\}. \tag{11}$$

Consider a pilot signal is inserted intentionally into the signal of CR system in terms of the duplication method described in (5), that is to say, a known pilot signal of PU, $S^p_{j,l}$, is reproduced to $S^c_{k,l}$ of CR signal. Thus, through the cyclostationary examination in (4), the SCF test of the signals received by the active-sensing node will be

$$\Gamma_r^{k-j} = \overline{R}_j \cdot \overline{R}_k^{\,*}. \tag{12}$$

Because it is impossible either to achieve global synchronization or to compensate for the overall phase rotation. As a result, we decided to take the magnitude to eliminate phase uncertainty of unsynchronized OFDM signals. Therefore, under $\mathcal{H}_1$, the test statistic $\mathcal{T}(R)$ becomes

$$\mathcal{T}(R)\mid_{\mathcal{H}_1} = \mid \overline{R}_j \cdot \overline{R}_k^{\,*}|^2. \tag{13}$$

By combining equation (13) with (11) and assuming that the effect of interference $\hat{I}$ is small, we can approximate equation (13) into

$$\begin{aligned}\mathcal{T}(R)\mid_{\mathcal{H}_1} \approx |&\hat{S}^p_j\hat{S}^{p\,*}_k + \hat{S}^p_j\hat{S}^{c\,*}_k + \hat{S}^c_j\hat{S}^{p\,*}_k + \hat{S}^c_j\hat{S}^{c\,*}_k \\ &+\hat{S}^p_j\hat{W}_k^{\,*} + \hat{S}^c_j\hat{W}_k^{\,*} + \hat{W}_j\hat{S}^{p\,*}_k + \hat{W}_j\hat{S}^{c\,*}_k + \hat{W}_j\hat{W}_k^{\,*}|^2.\end{aligned} \tag{14}$$

In equation (14), we find that the pilot signal $\hat{S}^p_j$ and the random sequence $\hat{S}^p_k$ are statistically uncorrelated, as are $\hat{S}^c_j\hat{S}^{c\,*}_k$ and $\hat{S}^c_j\hat{S}^{p\,*}_k$. Assume the noise $\hat{W}$ is small, thus, the main force of the test statistic under $\mathcal{H}_1$ will be the $\hat{S}^p_j\hat{S}^{c\,*}_k$ term, which is the intentional cyclostationary feature we embedded. It is clear that the sensing performance depends on the product of $\hat{S}^p_j$ and $\hat{S}^{c\,*}_k$; even if the signal strength of the PU network ($\hat{S}^p_j$) is very low, the detector can still provide good detection performance if the signal power of the CR network ($\hat{S}^c_k$) is well controlled. We are now in the position to say that the stated above shows how the interference from the CR network, $\hat{S}^c_k$, can be beneficial for detecting PU networks.

IV. Analysis

A. Detection Performance

The behavior of a detector can be modeled as a test of a binary hypothesis illustrated in equation (1). To completely characterize the impact of noise and interference level on the performance of active sensing, the detection and false alarm probability, used for appraising a detector, should also be examined. This section provides an analysis of our work in terms of the false alarm probability and detection probability. The test statistic of the detector under the condition $\mathcal{H}_0$ is

$$\begin{aligned}\mathcal{T}(R)\mid_{\mathcal{H}_0} &= |\overline{R_j}\cdot\overline{R_k}^*|^2 \\ &= |\{\hat{S}_j^c+\hat{I}_j+\hat{W}_j\}\cdot\{\hat{S}_k^{c*}+\hat{I}_k^*+\hat{W}_k^*\}|^2. \end{aligned}\quad (15)$$

Under the assumption that the effects of interference term $\hat{I}$ is small, we can get:

$$\mathcal{T}(R)\mid_{\mathcal{H}_0} \approx |\hat{S}_j^c\hat{S}_k^{c*}+\hat{S}_j^c\hat{W}_k^*+\hat{W}_j\hat{S}_k^{c*}+\hat{W}_j\hat{W}_k^*|^2. \quad (16)$$

The test statistic $\mathcal{T}(R)\mid_{\mathcal{H}_0}$ is a random variable whose PDF is a chi-square distribution with K degrees of freedom, where K is the number of features that we summed. If W_k is circularly symmetric complex Gaussian, using the central limit theorem for a large K, the PDF of $\mathcal{T}(R)$ can be approximated by a Gaussian distribution $\mathcal{CN}(\mu_0,\sigma_0^2)$ with

$$\mu_0 = K\left(\frac{\sigma_{\hat{c}}^2+\sigma_{\hat{W}}^2}{M}+\frac{\sigma_{\hat{c}}^2\sigma_{\hat{W}}^2+\sigma_{\hat{W}}^4}{M^2}\right) \quad (17)$$

and

$$\begin{aligned}\sigma_0^2 = K\Big(&\frac{\sigma_{\hat{c}}^4+2\sigma_{\hat{c}}^2\sigma_{\hat{W}}^2+\sigma_{\hat{W}}^4}{M^2}+\frac{4\sigma_{\hat{c}}^4\sigma_{\hat{W}}^2+4\sigma_{\hat{c}}^2\sigma_{\hat{W}}^4+4\sigma_{\hat{W}}^6}{M^3}\\ &+\frac{3\sigma_{\hat{c}}^4\sigma_{\hat{W}}^4+3\sigma_{\hat{W}}^8+4\sigma_{\hat{c}}^2\sigma_{\hat{W}}^6}{M^4}\Big)\end{aligned} \quad (18)$$

For a given threshold λ, the probability of a false alarm is

$$P_{FA}(\lambda) = p_r(\mathcal{T}(R)>\lambda \mid \mathcal{H}_0) = \mathcal{Q}((\lambda-\mu_0)/\sigma_0)$$

where $\mathcal{Q}(\cdot)$ is the area under the tail of a Gaussian PDF. From (16), for a desired false alarm probability $\hat{P}_{FA}$ of a sensing node, the corresponding detection threshold $\lambda(\hat{P}_{FA})$ can be evaluated by

$$\lambda(\hat{P}_{FA}) = \sigma_0\cdot\mathcal{Q}^{-1}(\hat{P}_{FA})+\mu_0. \quad (20)$$

Similarly, according to equation (14) and using central limit theorem, the PDF of test statistic under $\mathcal{H}_1$ can also be approximated by a complex Gaussian distribution $\mathcal{CN}(\mu_1,\sigma_1^2)$ with

$$\mu_1 = K\left(1+\frac{\sigma_{\hat{c}}^2+\sigma_{\hat{p}}^2+2\sigma_{\hat{W}}^2}{M}+\frac{\sigma_{\hat{c}}^2\sigma_{\hat{p}}^2+\sigma_{\hat{c}}^2\sigma_{\hat{W}}^2+\sigma_{\hat{p}}^2\sigma_{\hat{W}}^2+\sigma_{\hat{W}}^4}{M^2}\right) \quad (21)$$

$$\begin{aligned}\sigma_1^2 = K\Big(&\frac{2\sigma_{\hat{c}}^2+2\sigma_{\hat{p}}^2+4\sigma_{\hat{W}}^2}{M}\\ &+\frac{\sigma_{\hat{c}}^4+\sigma_{\hat{p}}^4+4\sigma_{\hat{c}}^2\sigma_{\hat{p}}^2+6\sigma_{\hat{c}}^2\sigma_{\hat{W}}^2+6\sigma_{\hat{p}}^2\sigma_{\hat{W}}^2+6\sigma_{\hat{W}}^4}{M^2}\Big)\end{aligned} \quad (22)$$

Therefore, the detection probability for a chosen threshold λ is given by

$$P_D(\lambda) = p_r(\mathcal{T}(R)>\lambda \mid \mathcal{H}_1) = \mathcal{Q}((\lambda-\mu_1)/\sigma_1). \quad (23)$$

B. Sensing-Throughput tradeoff

In general, the more the intentional cyclostationary feature is embedded, the more agile and accurate the CR systems would be in detecting PU networks. However, there is a trade-off between the number of embedded features and the throughput of the CR network. Recall the signal frame structure in Fig. 1(b), the achievable throughput of CR system denoted by $\mathcal{C}$ can be expresses as

$$\mathcal{C} = P(\mathcal{H}_0)\cdot c_0\cdot(N-\frac{K}{2})(1-P_{FA}(\lambda)) \quad (24)$$

where c_0 is the achievable throughput of each subcarrier, $P(\mathcal{H}_0)$ is the probability that PU signal is absent, and N is the total number of subcarriers of the CR system. Clearly, the equation (24) indicates that the number of features K and the false-alarm probability $P_{FA}(\lambda)$ have major effect on achievable throughput of CR systems. However, $P_{FA}(\lambda)$ is a function of K and they are in a tradeoff relation. Despite of the tradeoff, the CR base station may adjust the parameters of the intentional cyclostationary features according to the requirements of the PU network's protection or the demands of CR network's data transmission.

V. Simulation Results

To test and demonstrate the presented concept for active sensing, we use a DVB-T 2K mode for PU networks, and an OFDM system similar to DVB-T with 2048 subcarriers is adopted as the CR system in our simulations. The PU and CR networks are operating in the same radio band. In the simulation, total K pilots were intentionally inserted into each OFDM symbol of CR signals; M OFDM symbols were averaged in each test. An ordinary cyclostationary feature detector [7] which detects the inherent features of PU's signal and has the best sensing capability of other common detectors is chosen to compare the sensing performance with our method. The signal-to-noise ratio (SNR) is defined as the ratio of the PU's signal power and the noise power at the active-sensing node. Likewise, the signal-to-interference-plus-noise ratio (SINR) is defined as the ratio of the PU's signal power and the noise power plus the interference power, where the interference component refers to the CR's signal power.

In Fig. 4, in terms of the relationships among the detection probability and the false alarm probability, the results show a striking effect of the proposed signal structure on active sensing performance. The solid lines represent active sensing with the proposed signal structure; the dotted lines represent the active sensing on inherent features of the PU's signals using an ordinary cyclostationary feature detector. Where the SNR is set to 0dB and the SINR is -12dB. The results indicated that co-channel interference from CR networks has negative effect on the performance of active sensing; an ordinary cyclostationary feature detector cannot provide robust active sensing.

The curves in Fig. 5 present the detection performance of active sensing under the AWGN channel, where the false alarm probability is 0.01, SNR is 0dB, and SINR is -10dB. Compared

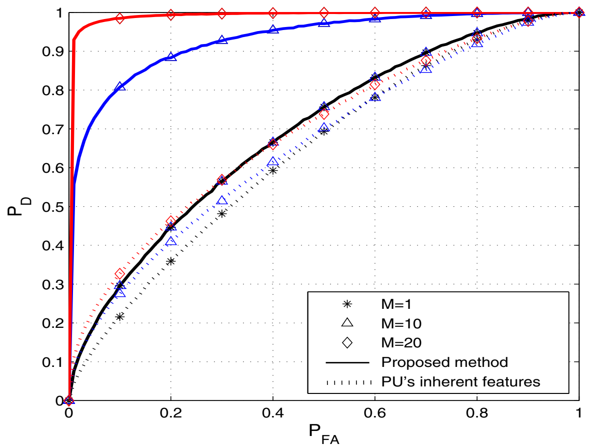

Fig. 4. False alarm probability vs. detection probability. AWGN channel, SNR = 0dB, SINR = -12dB, M = 1, 10, and 20.

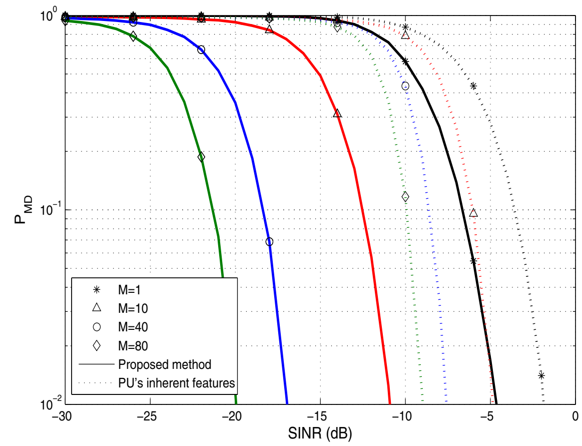

Fig. 5. Mis-detection probability vs. SINR. AWGN channel, P_{FA} = 0.01, SNR = 0dB, M = 1, 10, 40, and 80.

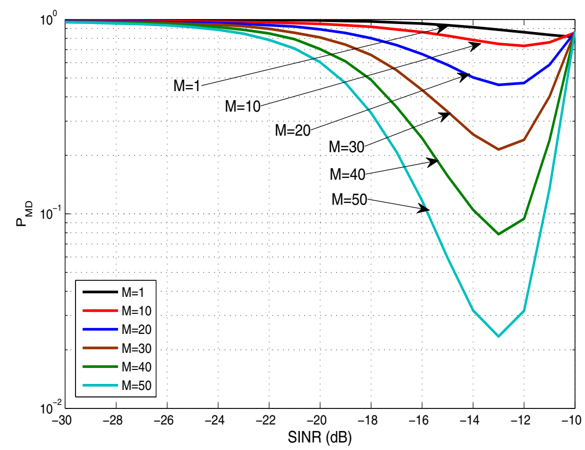

Fig. 6. Mis-detection probability vs. SINR. AWGN channel, P_{FA} = 0.01, SNR = -10dB, M = 1, 10, 20, 30, 40, and 50.

with the method of detecting the PU's inherent features by an ordinary feature detector, the proposed signal structure is more robust to co-channel interference. Fig. 6 shows an additional advantage of the proposed method. In this experiment, we set the SNR to -10dB and varied the interference power (CR's signal power). Generally speaking, the miss-detection probability is high when the PU's signal power is weak (e.g., M is 40 as SNR is -10dB and SINR is -10dB). However, by increasing the interference power (e.g., M is 40 as SNR is -10dB and SINR is -13dB), we can improve the detection performance of active sensing. This result verifies the analysis in equation (14), and it may provide new insight and more innovative possibilities for active sensing of CR.

VI. Conclusion

A new signal structure for active sensing in CR communications has been proposed. The proposed technique, which is based on the principle of cyclostationary signature design, involves duplicating the pilot information of the PU's signal and embedding it into the CR signal. In doing this, the intentional similarity feature is presented when both PU and CR networks are active. The proposed structure gives us satisfactory results under low SNR and low SINR. Compared with the conventional active sensing method trying to detect the inherent feature in the PU's signal, the proposed approach achieves much better detection performance under the same sensing time which in terms of M. The simulation results also show that the proposed scheme has a shorter sensing time, by approximately 1/10, in achieving the same performance as the conventional method when the SINR is -5dB and the SNR is 0dB.

Acknowledgment

This work was supported by the National Science Council of the Republic of China under Grant NSC 99-2221-E-007-016-MY3.

References

[1] J. Mitola III, "Cognitive radio: An integrated agent architecture for software defined radio," Ph.D. Thesis, Royal Institute of Technology Stockholm, Sweden, 8 May, 2000.

[2] IEEE 802.22, Working Group on Wireless Regional Area Networks (WRAN), http://grouper.ieee.org/groups/802/22/.

[3] Y.-C. Liang, Y. Zeng, E. Peh, and A. T. Hoang, "Sensing-throughput tradeoff for cognitive radio networks," *IEEE Trans. Wireless Commun.*, vol. 7, no. 4, pp. 1326-1337, Apr. 2008.

[4] S. Stotas and A. Nallanathan, "Overcoming the sensing-throughput trade-off in cognitive radio networks," in *Proc. of IEEE Int. Conf. Commun. (ICC '10)*, Cape Town, South Africa, May 2010, pp. 1-5.

[5] Y. L. Hsieh, S. H. Song, and Q. T. Zhang, "Active sensing for cognitive radio," in *IEEE 70th Veh. Technol. Conf. (VTC '08)*, Anchorage, USA, Sept. 2009, pp. 1-5.

[6] S. H. Song, K. Hamdi, and K. B. Letaief, "Spectrum sensing with active cognitive systems," in *IEEE Trans. Wireless Commun.*, vol. 9, no. 6, pp. 1849-1854, Jun. 2010.

[7] W. Gardner, "Signal interception: a unifying theoretical framework for feature detection," *IEEE Trans. Commun.*, vol. 36, no. 8, pp. 897-906, Aug. 1988.

[8] P. D. Sutton, K. E. Nolan, and L. E. Doyle, "Cyclostationary signatures in practical cognitive radio applications," in *IEEE Journal on Selected Areas in Communications*, vol. 26, no. 1, pp. 13-24, Jan. 2008.